Development of Concentric Vapor Chambers for Heating and Cooling of Advanced Sorption Systems

Elizabeth Seber[1] and Michael C. Ellis.[2]
Advanced Cooling Technologies, Inc., Lancaster, PA, 17601

Within the closed-system environment of the International Space Station (ISS), sufficient removal of carbon dioxide (CO_2) is vital for life support efforts. Ideally, the removed CO_2 would also serve a purpose within the station. The Air-Cooled Temperature Swing Adsorption Compressor (AC-TSAC) is one such novel system that captures CO_2 from the ISS cabin air using a sorbent material. The CO_2 is then released from the sorbent material when heated up, which also works to compress the released gas. This high-pressure CO_2 can then be delivered to other systems within the ISS, such as a Sabatier reactor. The release of CO_2 recharges the sorbent material, allowing the sorbent to begin the adsorption cycle anew. The AC-TSAC operates with two beds, operating in offset cycles such that there is uninterrupted CO_2 adsorption and delivery. These beds need a high degree of thermal control, first to heat up to release the CO_2 and pressurize, and second to cool down rapidly to restart the adsorption cycle. This swing of temperatures needs to be uniform throughout the bed to ensure optimal efficiency of the AC-TSAC sorbent bed. Typical sorbent materials, such as zeolite, have notoriously poor heat transfer characteristics, so a thermal control system must be well integrated into the bed while taking up as little size, weight, and power (SWaP) as possible. Under a NASA Phase II SBIR Program, ACT has developed and compared four potential vapor chamber designs for the AC-TSAC, improving on initial Phase I Designs and adapting the technology to operate within the AC-TSAC's adsorption/compression cycle. The design process is discussed in depth, alongside modeling results describing the temperature profile of the AC-TSAC sorbent bed. The vapor chamber designs were compared based on achieving better temperature uniformity in the sorbent bed, higher average temperatures, and manufacturability.

Nomenclature

4-AVC	=	Four-Arc Vapor Chamber
7HP	=	Seven Heat Pipes
ACT	=	Advanced Cooling Technologies
AC-TSAC	=	Air-Cooled Temperature Swing Adsorption Compressor
AVC	=	Annular Vapor Chamber
CDRA	=	Carbon Dioxide Removal Assembly
CO_2	=	Carbon Dioxide
ISS	=	International Space Station
NASA	=	National Aeronautics and Space Administration
SOTA	=	State-of-the-Art
SSVC	=	Star-Shaped Vapor Chamber
SWaP	=	Size, Weight, and Power
TMS	=	Thermal Management System
VC	=	Vapor Chamber

[1] R&D Engineer II, Research & Development, 1046 New Holland Avenue, Lancaster, PA 17601, USA.
[2] Senior Engineer, Research & Development, 1046 New Holland Avenue, Lancaster, PA 17601, USA.

I. Introduction

THE Carbon Dioxide Removal Assembly (CDRA) is a critical component used on the International Space Station (ISS) as part of the air revitalization system[1]. Cabin air is pumped through a sorbent bed within the CDRA, and carbon dioxide (CO_2) is selectively captured by the sorbent material (typically a zeolite). Once the bed reaches capacity, the material is heated up to cause the release of CO_2, which is then driven outside the ship as a waste product. In an evolution of this life support technology, the Air-Cooled Temperature Swing Compression System (AC-TSAC) was designed to perform the same capabilities as the CDRA, while also maximizing the amount of CO_2 collected by using a dual-bed system with a temperature swing cycle to alternate adsorption and release. The collected CO_2 is pressurized when released and used within a Sabatier reactor, rather than being ejected[2]. A model of a CO_2 capture bed is shown in Figure 1.

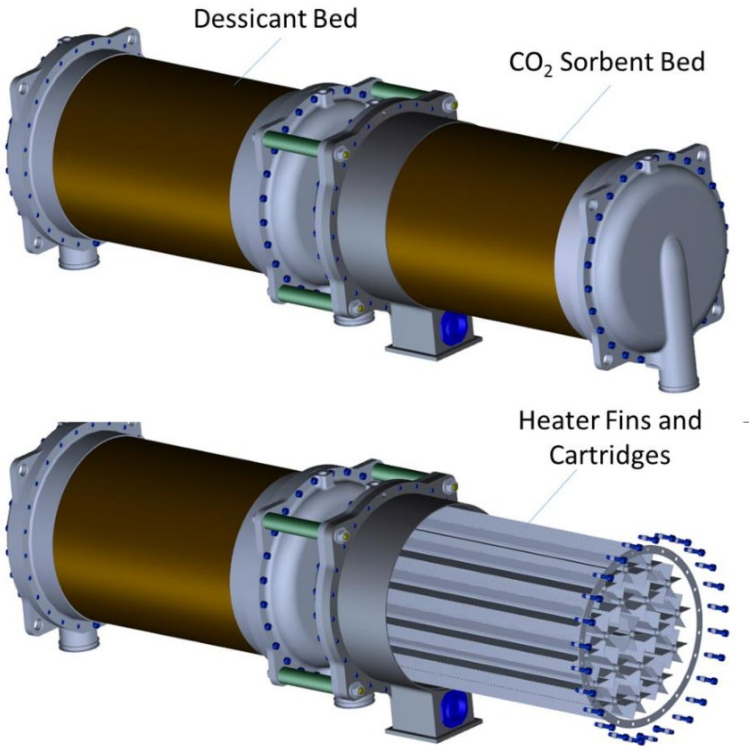

Figure 1. CO_2 Capture Bed[5].

The temperature swing cycle of each bed contains four phases: Adsorption, Compression, Production, and Cooling. Zeolite selectively adsorbs CO_2 at moderate temperatures and low pressures, (less than 25 °C and 200 torr), and so during the adsorption stage, low-pressure, dry cabin air is blown through the sorbent bed[2]. To release the adsorbed CO_2 and reset the sorbent bed, the zeolite must be heated up to 200 °C. In the compression stage, connecting valves are closed and the thermal management system (TMS) heats the bed. Once the bed reaches 200 °C, the released CO_2 builds up in pressure as the bed temperature continues to rise. During the production stage, the outlet valve is opened, and a high-purity CO_2 stream leaves the bed. Afterward, the bed is cooled down during the cooling phase and is ready to absorb again.

This entire cycle is temperature-dependent, so controlling the temperature of the zeolite is critical for operation. The considerably low thermal conductivity of Zeolite (ranging from approximately 0.6 to 4 W/m•K) [3] compared to a common TMS envelope material like aluminum's thermal conductivity (160 W/m•K)[4] necessitates a robust TMS design. This TMS must transfer thermal energy evenly and quickly to the zeolite to release the adsorbed CO_2 but must also not occupy too much volume in the size-limited sorbent bed. The TMS must also rapidly cool down the zeolite to reset the cycle. Systems with low size, weight, and power (SWaP) properties are highly desired for space applications. As such, this research seeks to design a TMS that optimally heats the sorbent bed while minimizing the required SWaP. The design work presented here represents the first steps in design optimization through modeling the

thermal conductance across a cross-section of the sorbent bed. Given that the main challenge for the TMS will be uniform heating, only the heating periods (compression and production) are explored in this paper.

II. State-of-the-Art Thermal Management System

The research presented in this paper reflects the design improvements made in a Phase II NASA SBIR program. At the time of the Phase I effort, the state-of-the-art (SOTA) for heating and cooling zeolite was a circular tube that held a cartridge heater, inserted into the 12 in. length of the sorbent bed. This tube had six axial fins with a tip-to-tip length of 1.75 in., creating a star-shaped profile, made of aluminum. This design held several problems, with the largest problem being the temperature gradient along the fins resulting in non-uniform zeolite temperatures.

To improve upon this design, ACT fabricated a star-shaped vapor chamber (VC) during the Phase I SBIR Effort, which innately has a higher thermal conductivity compared to aluminum[6]. Both the SOTA and ACT's Star-Shaped VC are shown in Figure 2. Vapor chambers are passive heat transfer devices that can transport high amounts of thermal energy by taking advantage of two-phase heat transfer, much like heat pipes. ACT demonstrated through testing that the integration of vapor chambers into the sorbent greatly improved the thermal conductivity of the TMS and the thermal uniformity of the zeolite. The star-shaped vapor chamber showed several other improvements over the SOTA but required many internal support structures to withstand the pressures of the internal working fluid when heated to 200 °C. These added structural considerations increased the size and weight of the star-shaped vapor chamber. Considering this, ACT identified a need to reconsider the star-shaped geometry of the vapor chamber for one that does not require as much structural material, while still delivering on thermal performance.

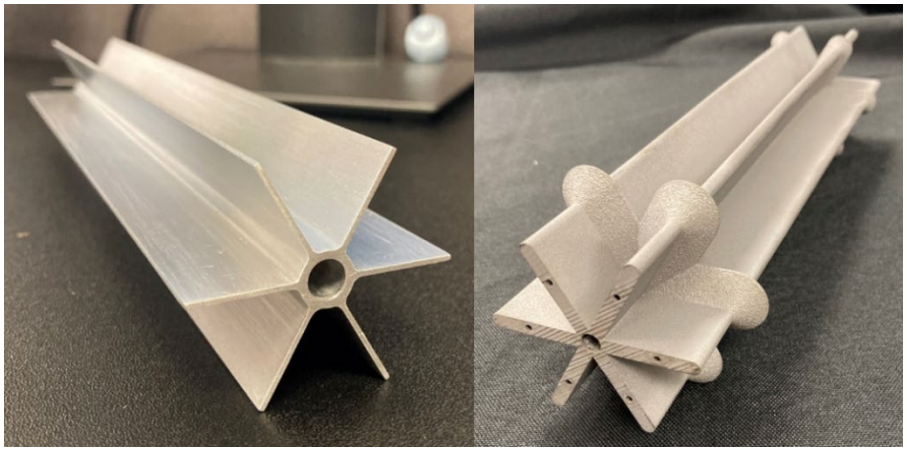

Figure 2. Left: NASA's SOTA Heater with Axial Fin, tip-to-tip fin length is 1.75 in.; Right: ACT's Star-Shaped Vapor Chamber, tip-to-tip fin length is 1.85 in. The total depth of each is 12 in.

A similar design effort was previously performed by NASA Ames Research Center to optimize the thermal performance of the AC-TSAC and investigated cylindrical and rectangular bed geometries and the use of aluminum plates vs. vapor chambers for conducting heat through the bed[7]. The study found that the use of vapor chambers improved the viability of a cylindrical bed, which is desirable due to the form factor and potential for uniform heat spreading. The structural design of these vapor chambers was not examined in the study, but cylindrical vapor chambers are structurally stronger than flat plate, rectangular vapor chambers, resulting in less material needed for the envelope material. Additionally, the study found that when heaters are placed on the exterior shell of the bed, the conduction through the cylindrical bed lowered as heat had to first pass through the low-conductivity zeolite before reaching the vapor chambers. ACT's bed design integrates the heaters into the vapor chambers, negating this design flaw.

III. Thermal Modeling Design Study

A. Vapor Chamber Geometries

Several geometric shapes of vapor chambers were identified for modeling and comparison, the cross-sections of which are shown in Figure 3. Rather than modeling performance across the entire 8-in. diameter cylindrical bed, a unit cell of the different geometries was created. This unit cell is 4-in. in diameter and maintains the 12-in. bed depth.

The geometries examined include an array of seven heat pipes (7HP), ACT's star-shaped vapor chamber (SSVC), an annular vapor chamber with a single central heat pipe (AVC), and an annular vapor chamber sectioned into four arcs with a single central heat pipe (4-AVC). The selected geometries were not individually optimized for their shape but were selected to show an array of possible geometries, building off of prior works, and their differences in performance. To directly compare the shapes, the vapor chambers could not extend 1.05 in. from the center of the 4 in. diameter bed, and the maximum thickness/diameter for each geometry was 0.25 in.

The maximum volume of the AC-TSAC bed volume is constrained, so reducing the size of the vapor chambers is a critical design goal for this design study. Since each bed run in this simulation is 12 in. long, the cross-sectional area for each vapor chamber model was recorded, rather than volume, and is described in Table 1. The maximum possible cross-sectional area of the zeolite bed with no embedded vapor chambers is 12.57 in^2. The shape that took the least cross-sectional area, and therefore also took the least amount of sorbent volume away from the bed, was the array of seven heat pipes with a cross-sectional area of 0.35 in^2. The 7HP model also had the least amount of surface area in contact with the zeolite (5.53 in. perimeter), which limits the heat transfer capabilities of the model. Conversely, the shape that took the most volume away from the bed was the annular vapor chamber (1.5 in^2). The AVC also had the highest surface area in contact with the zeolite, with a perimeter of 12.41 in. The SSVC and 4-AVC models fell in the middle, with moderate volume removed from the bed and moderate perimeters. From a volume vs. surface area contact perspective, these two models are the most promising, yet the behavior of the conduction through the bed must be explored to determine the performance.

Table 1. Geometric comparison of selected vapor chamber shapes.

Vapor Chamber Geometry	Cross-Sectional Area of VC [in^2]	Cross-Sectional Area of Zeolite [in^2]	Perimeter of VC [in]
No Vapor Chambers	-	12.57	-
Seven Heat Pipes	0.35	12.22	5.5
Star-Shaped Vapor Chamber	1.39	11.18	10.45
Annular Vapor Chamber	1.5	11.06	12.41
Four-Arc Vapor Chambers	1.14	11.43	10.25

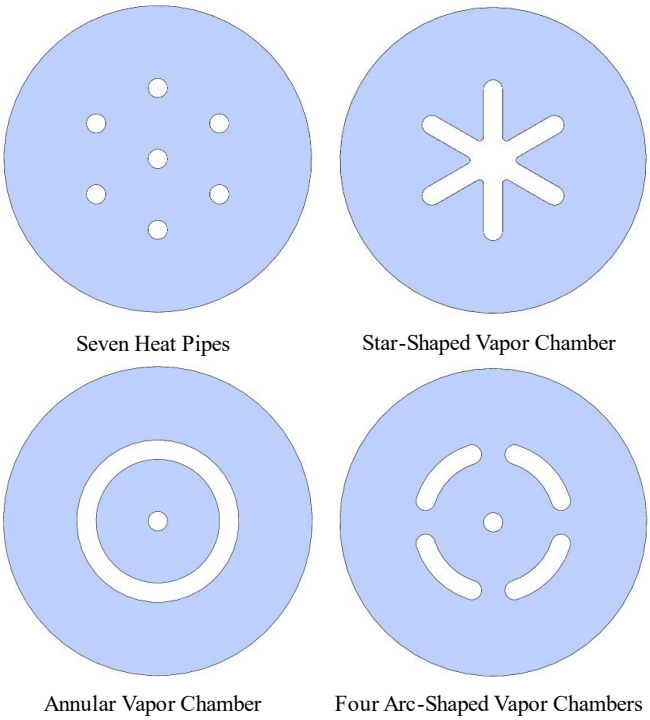

Figure 3. Cross-sections of models tested.

B. Modeling Methodology

The focus of this modeling effort was to examine how the selected geometries affect heat transfer throughout the bed, with the goal of the most uniform bed temperature with the least amount of volume taken up by the vapor chamber. A transient thermal conduction simulation was run for each shape to simulate the compression stage of the temperature swing cycle. The conduction simulation was done with SolidWorks Simulation. This simulation used a two-dimensional simplification, with a twelve-inch projection representative of the bed depth. The vapor chambers were treated as a void within the zeolite bed, the perimeter of which was given a convection coefficient to represent the high thermal conductivity of the vapor chamber. Each vapor chamber is assumed to have a cartridge heater supplying the thermal load. The initial temperature of the zeolite was sent to 20 °C to reflect the temperature of the bed at the beginning of the compression stage. The simulation was run for 600 s to reflect the duration of this stage as identified in Ref. 2, and a time step of 1 s was selected.

Parameters that were held consistent across the studies include the material properties of the zeolite, the duration and time-step of the simulation, the initial temperature of the bed, the convection coefficient of the vapor chambers, and the corresponding bulk temperature of the vapor chamber. Thermal loads and boundary conditions for the simulations are depicted in Figure 4, using the 7HP shape model as an example.

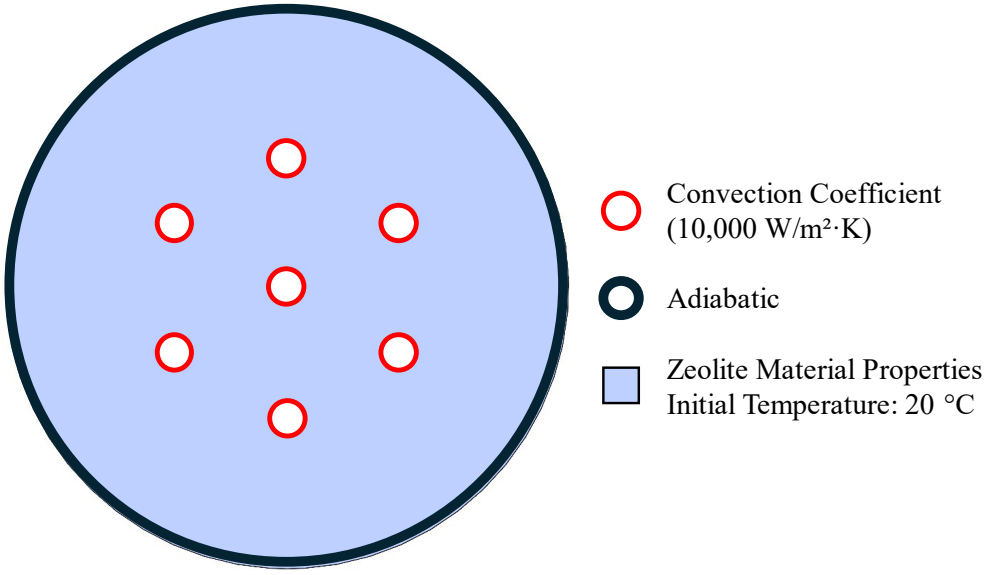

Figure 4. Labeled cross-section of the 7HP model to show the conduction simulation boundary conditions.

IV. Modeling Results and Discussion

The transient conduction simulation resulted in a temperature plot across the two-dimensional surface of the sorbent bed models. A temperature-gradient plot for each model at the final time step (t=600 s) is shown in Figure 5, with the color scale for each model equally set to a range of 30-230 °C. Qualitatively, this visualization of temperature gradients provides insight into how the heat spreads from each vapor chamber shape through the sorbent material and helps interpret the raw temperature data. The seven-heat pipe model has a largely even temperature spread but at a lower temperature compared to the temperature spread in the annular and four-arc vapor chamber models. The star-shaped vapor chamber shows higher-temperature sorbent at the inner corners of the vapor chamber yet has a very sharp temperature gradient between the fins. Within the circular bed, the AVC has the most uniform, circular heat spread, followed closely by the 4-AVC. The heat pipe array and star-shaped vapor chamber each have a non-uniform temperature profile.

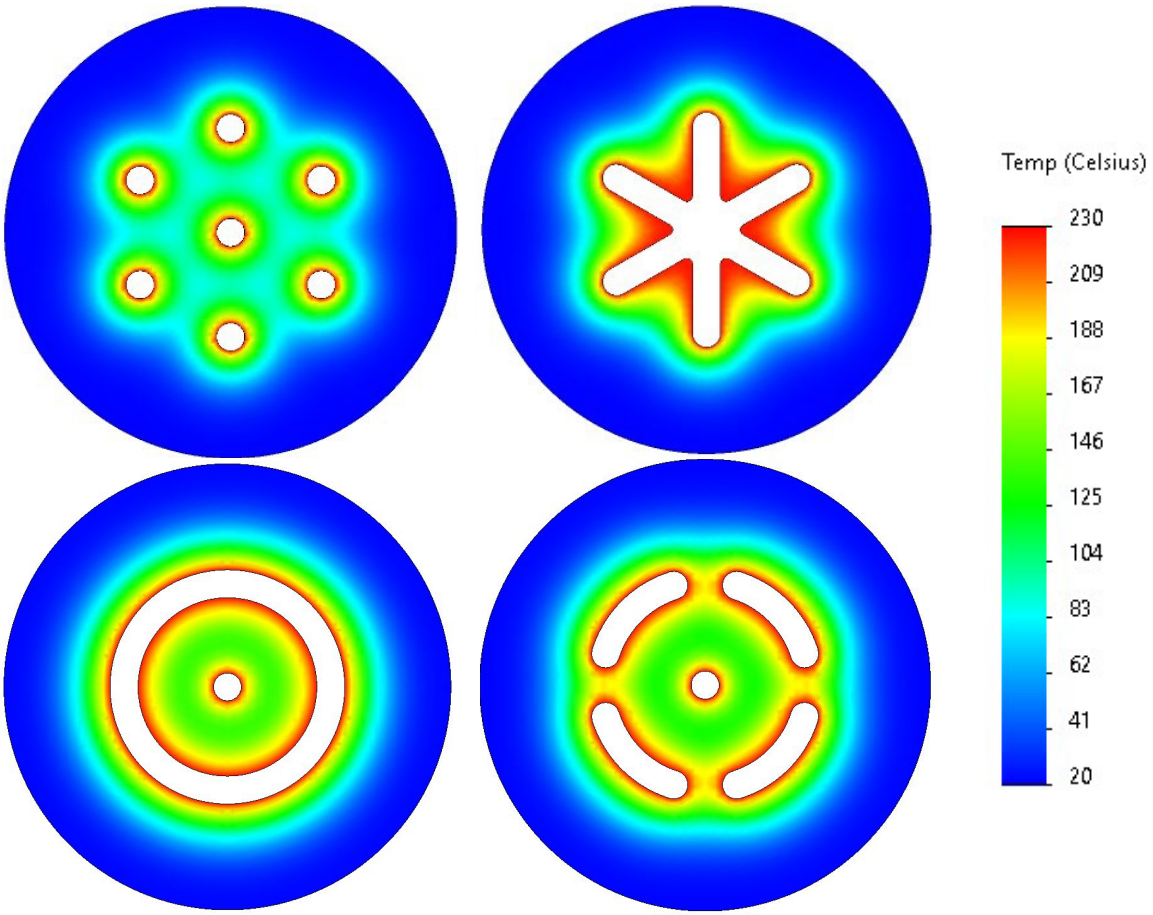

Figure 5. Temperature-gradient of sorbent at t = 600 s for each VC model cross-section.

Key temperatures and the standard deviation of collected data from the final time step (t=600 s) are shown in Table 2. Standard deviation was calculated using the temperature recordings at all nodes formed from the mesh. The mesh for each model was adequately uniform resulting in over 5,000 temperature readings for each model. For the data range encompassing the full 4 in. bed, each model had the same maximum temperature (227 °C), which was recorded at the interface between the vapor chamber and sorbent. The minimum temperature experienced by each model was around 20 °C, the initial temperature of the model, around the outer edges of the model. If the simulation was run for a longer duration, the minimum temperature would likely rise as heat slowly spreads through the sorbent. The vapor chambers could also be extended closer to the edge of the bed, or the array could be extended, to improve the overall temperature spread throughout the unit, but this optimization is outside the scope of this study.

From the temperature gradient plot seen in Figure 5, each simulation resulted in a highly isothermal ring around the edge of the bed. To better examine the temperature uniformity for each model, temperature data that fell within a 3-in. diameter area centered in the model was selected, an area 56% the size of the original bed area. The key temperatures and standard deviation of this data set are shown in Table 2. The maximum temperatures of the two data sets do not change, but the minimum temperatures rise as the area of data collection is tightened. The average temperatures for the reduced data set rise significantly, and more accurately represent the average temperature of the vapor chambers within the area of interest. Higher maximum and average temperatures are desirable as the goal is for the bed to reach 200 °C to release CO_2 from the zeolite. A lower standard deviation is desired and demonstrates a higher degree of temperature uniformity, indicating a maximum utilization of the zeolite.

The standard deviation of the 7HP model dropped slightly (51.27 °C to 49.52°C), and the SSVC standard deviation raised slightly (66.68 °C to 67.93 °C). The AVC and 4-AVC models had a significant decrease in standard deviation, nearly 13 °C difference for each. This indicates that within the area of interest, these models have very high-temperature uniformity, comparable to the 7HP model.

Table 2. Key temperatures and standard deviation at t = 600s for each vapor chamber geometry.

	Seven Heat Pipes	Star-Shaped Vapor Chamber	Annular Vapor Chamber	4-Arc Vapor Chamber
Full Bed Area (4 in. Diameter)				
Maximum Temperature [°C]	227	227	227	227
Minimum Temperature [°C]	20.1	20.1	21.2	20.6
Average Temperature [°C]	61.986	69.43	84.65	84.44
Standard Deviation [°C]	51.27	66.68	68.73	68.51
3 in. Diameter				
Maximum Temperature [°C]	227	227	227	227
Minimum Temperature [°C]	25.6	26.1	49.9	39.3
Average Temperature [°C]	94.75	114.34	141.31	137.7
Standard Deviation [°C]	49.52	67.93	54.35	55.32

The average temperature for each bed versus time is shown in Figure 6. In this figure, the AVC and the 4-AVC have nearly identical average temperatures throughout the transient simulation. The 7HP model showed the lowest average temperature. Both the AVC and 4-AVC showed consistently higher average temperatures, reaching 14 °C above the SSVC and 23 °C above the 7HP model by the final time step. In comparing this data to the temperature gradient plot in Figure 5, we can see that the heat spread between the AVC and 4-AVC is comparable to the 7HP Model, the temperatures are on average higher, likely due to the increase in surface area available for heat transfer.

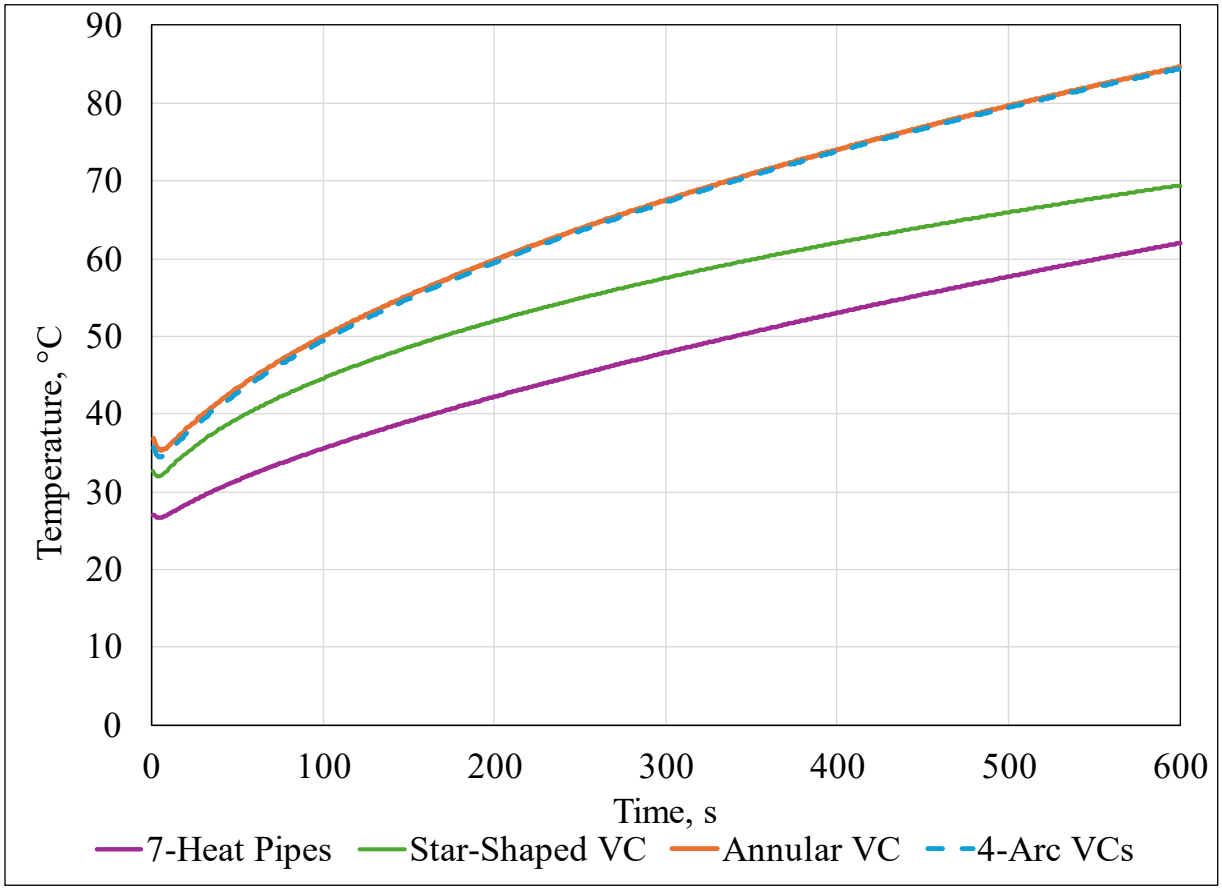

Figure 6. Time vs. Average Sorbent Temperature for each vapor chamber model.

Out of the four vapor chamber geometries modeled the Seven Heat Pipe array had the lowest overall size, and lowest temperature deviation, indicating higher temperature uniformity. The 7HP model also had the lowest average temperature. As a result, this model would require more power and time to heat the entire bed to 200 °C, the desired temperature for releasing and pressurizing CO_2 from the zeolite. This trade-off may negate the benefits of a uniformly heated bed in favor of a lower-power, faster-performing system.

The Star-Shaped Vapor Chamber had the second lowest overall size, as well as the second lowest temperature and temperature deviation. Given that the temperature deviation data range included the large, nearly isothermal room-temperature ring around the exterior edge of the bed, likely, this standard deviation does not adequately reflect the sharp temperature gradient occurring between the fins of the SSVC.

The Annular Vapor Chamber and 4-Arc Vapor perform very similarly. Both models showed the highest average temperature and comparably lower temperature deviation, and yet the 4-AVC does so with 24% less cross-sectional area. Therefore, the sectioning of the annular vapor chamber into arc segments allowed for the same high conductivity in the bed while reducing the size and weight of the vapor chambers.

V. Conclusion and Future Work

ACT completed a geometric design study comparing state-of-the-art vapor chambers to novel vapor chamber shapes to increase the temperature uniformity of sorbent material while decreasing the size and weight of the thermal management system. This work suggests that the use of four, arc-shaped vapor chambers is an optimal vapor chamber shape for low-conductivity sorbent beds due to the improved temperature uniformity, improved heat distribution, and reduced size when compared to the alternate geometries presented. The heat pipe array and annular vapor chambers do not require the internal structural supports that the star-shaped vapor chamber does and can result in less overall weight of the thermal management system.

Complementary research on CO_2 adsorbent beds investigated additive manufacturing of the sorbent material, focusing on maximizing surface area to interact with and capture CO_2 while minimizing pressure drop across the bed to reduce the pumping power required to run air through the bed[8]. This manufacturing method would maximize the performance of the sorbent material. The heat pipe array, annular vapor chamber, and segmented arc vapor chamber are ideal shapes for integrating the thermal management system with the printed zeolite. A tight fit between the sorbent material and the vapor chamber is desirable to improve the thermal conductivity across the bed and to prevent airflow from bypassing the sorbent material around the edges of the material.

Further work must be done to develop novel vapor chamber shapes before they can be integrated into the AC-TSAC. The bed geometries modeled above reflect only a unit cell of the full-scale AC-TSAC, and so the designs must be increased in scale and further optimized. From there, the vapor chamber wick structure must be designed and optimized for additive manufacturing, and testing will need to occur to corroborate the modeling effort. ACT will accomplish much of this work throughout the NASA SBIR Phase II program from which this research was funded.

Acknowledgments

The authors acknowledge Haley Myer, Max Demydovych, and Megan Gettle for their work in designing and testing the Phase I Star-Shaped Vapor Chamber. The authors would also like to acknowledge the NASA SBIR Program (Contract No. 80NSSC23CA061) for financially supporting the project, and Tra-My Justine Richardson for her technical support and guidance as the Technical Program Manager.

References

[1] El Sherif, D. and Knox, J.C. "International Space Station Carbon Dioxide Removal Assembly (ISS CDRA) Concepts and Advancements," *35th International Conference on Environmental Systems,* 2005.

[2]Alcid, M., Gan, K., Richardson, T.-M. J., Jan, D. and Castellanos, D. "Air-Cooled Temperature Swing Compression System Rebuild", *50th International Conference on Environmental Systems,* 2021.

[3]Schnell, S. K., Vlugt, T. J. H., "Thermal Conductivity in Zeolites Studied by Non-equilibrium Molecular Dynamics Simulations," *International Journal of Thermophysics,* Vol. 34, 2013, pp. 1197-1213.

[4]Touloukian, Y.S., *Recommended Values of the Thermophysical Properties of Eight Alloys, Major Constituents and their Oxides*, Thermophysical Properties Research Center, Lafayette, Indiana, 1966, pp. 7.

[5]Schunk, R. G., Peters, W. T., and Thomas, Jr., J.T., "Four Bed Molecular Sieve Exploration (4BMS-X) Virtual Heater Design and Optimization," *47th International Conference on Environmental Systems,* 2017.

[6]Myer, H. E. and Ellis, M. C., "Novel Vapor Chambers for Heating and Cooling of Advanced Sorption Systems," *52nd International Conference on Environmental Systems,* 2023.

[7]Alpert, H. S., Peterson, K., Richardson, T.-M. J., Dzurny, Q., and Peterson, G. P., "Thermal Modeling of a Novel Air-Cooled Temperature Swing Adsorption Compressor (AC-TSAC)," *52nd International Conference on Environmental Systems,* 2023.
[8]Steppan, J., Hsu, J., Morikawa, K., Millet, B., and Meaders, T., "Additively Manufactured, Net-Shape Adsorbent Beds for Carbon Dioxide Removal," *51st International Conference on Environmental Systems*, 2022